# Stable and metastable InGaAs/GaAs island shapes and surfactant-like suppression of the wetting transformation

R. Leon*
*Jet Propulsion Laboratory, California Institute of Technology, 4800 Oak Grove Drive, Pasadena, CA 91109-80099*

C. Lobo
*Research School of Physical Sciences and Engineering, Australian National University, Canberra, ACT 0200, Australia.*

J. Zou, T. Romeo and D. J. H. Cockayne
*Electron Microscope Unit & Australian Key Centre for Microscopy and Microanalysis, The University of Sydney, NSW 2006, Australia*

ABSTRACT

Diverging behaviors are observed in the InGaAs/GaAs Stranski-Krastanow (S-K) island formation during vapor phase epitaxy: varying group V partial pressures gives different critical thicknesses for the onset of the S-K transformation, island surface coverages, ratios between coherent and incoherent islands, and dissimilar morphologies upon annealing. The later experiments show that island shape metastability can be observed for some growth conditions; and that high concentrations of small lens shaped islands can also be found in equilibrium if InGaAs surface energies are minimized. These findings lead to the conclusion that $AsH_3$ can raise surface energies in the growth of InGaAs on (100) GaAs, thus acting as an impurity-free "morphactant".

PACS: 68.35.Md, 85.30.Vw, 81.15.Gh, 61.16

Submitted

## INTRODUCTION

The importance of Stranski-Krastanow (S-K) coherent island formation as a mechanism for strain relaxation has been established in both Ge/Si [1] and InAs/GaAs [2,3] heteroepitaxy. Interest in S-K growth has been re-kindled by the first reports of these strained islands to make defect-free, self-assembled, InGaAs/GaAs semiconductor quantum dots (QDs) [4-6]. Since then, a large number of studies have focused on strain relaxation by island formation. An improved understanding of the varying and often competing mechanisms that result in different morphologies during island nucleation will determine the successful utilization of these islands in semiconductor zero-dimensional (0-D) structures. Island shapes, aspect ratios, morphologies, and coherence/incoherence all play a role into the electronic/optic/magnetic properties of self-forming semiconductor quantum dots.

Recent reports show ripening behavior during island formation in both Ge/Si and InGaAs/GaAs heteroepitaxy. An in-situ study of the evolution of growth in Ge/Si found an optimum range in uniformity [7], desirable for device applications, during the evolution to the stable dome shaped configuration. Other reports show the coexistence of different types of islands [8] and a shape transition from small pyramid-shaped islands to dome-shaped islands upon annealing [9]. In InGaAs/GaAs QD formation, ripening has also been observed upon annealing, which is partially suppressed by steps in miscut substrates [10].

The observation of ripening of S-K islands suggests that the small coherent islands used for QDs might be unstable or metastable, with obvious disadvantages for optoelectronic applications of these island-based devices. Determining if stable islands can be achieved is thus of both practical and fundamental interest.

Several studies using surfactants in the growth of Ge/Si have produced striking results, from the total suppression of the S-K transformation [11,12], to different critical thicknesses for such transformation [13] and different island shapes [14] with facetting

from lower energy surfaces. No equivalent studies exist for the InGaAs/GaAs system, however it is plausible that similar effects induced from unintentional surfactant-like species might explain the present controversy in the different shapes reported for InGaAs and InAs islands.

Kinetic barriers for island formation have been observed with suppression of island nucleation from low adatom diffusion length, thus accomplishing 2-D growth of InGaAs films at low temperature [15]. Here we report on a suppression of the S-K transformation; however our results can be better explained by an offset of the energetics driving the islanding transition. Annealing experiments done at high $AsH_3$ partial pressures concur with the observation of Ostwald ripening, but we also observe that small, high density, lens-shaped islands are unaffected by prolonged annealing in ambient conditions as long as "optimum" values of group V partial pressures are used during the island growth. These results establish that lens-shaped self-forming semiconductor quantum dots can be stable.

InGaAs/GaAs structures were grown by metalorganic chemical vapor deposition (MOCVD). Details of the growth of InGaAs on GaAs (100) [16], the use of graded growth rates to study the structural evolution of InGaAs S-K formation [17] and the control of island densities in QD growth by varying group V partial pressures [18] have been reported elsewhere. The nominal ternary composition of the islands is $In_{0.6}Ga_{0.4}As$ and the growth temperature was 550°C. After island growth, uncapped structures were cooled to room temperature in the growth chamber, maintaining the arsine partial pressures to 400°C. Force microscopy (FM) with etched silicon nitride tips gave statistical information on island sizes and concentrations. Plan view transmission electron microscopy (TEM) and high resolution scanning electron microscopy were also used to establish equivalencies between structural measurements and to obtain a better assessment of island shapes.

In Figure 1 shows the fractional surface coverage from nanometer size InGaAs islands. All conditions were the same with the exception of the Arsine partial pressures. Figure 1 shows statistics for two types of islands: small coherent islands used in quantum dot applications, and larger islands that are found to coexist with the QDs in different ratios. As is seen in figure 1, these ratios depend critically on growth conditions. Figure 2 shows a plan view TEM micrograph of uncapped InGaAs islands illustrating the coexistence of both types of islands. The larger islands are incoherent as evidenced by the presence of dislocations and Moiré patterns. The sample shown in the micrograph was grown under the Arsine partial pressure indicated by arrow (b) in figure 1. TEM observation of different islands grown at high arsine partial pressures show that the larger faceted islands are incoherent, containing dislocations within.

The plots with solid diamonds and circles in figure 1 show the respective average diameter and fractional surface coverage of these large islands, indicating that their density and sizes are dependent on arsine flow. As can be seen, the fractional coverage for the small islands (QDs) is significantly higher for an optimal value in Arsine partial pressures. Surface coverages for small islands change from a maximum of 25% for values of Arsine partial pressures near $10^{-6}$ to surface coverages of only 5% for partial pressures near $10^{-5}$. On the other hand, values for fractional coverages by large islands are high for conditions that promote low coverage from small islands, and reach almost 50% at high Arsine flows. These large islands also increase in size for conditions that promote low small island coverages. These results indicate that small islands are found in lower concentrations with growths at high Arsine partial pressures while the large incoherent island concentrations have opposite trends.

A different type of experiment is presented in figure 3. Depositions using a graded growth rate were performed for two different values of Arsine partial pressures. Gradients in quantum dot density can be produced with MOCVD by varying the carrier gas ($H_2$) flow. Numerical simulations of concentration profiles and QW emission energy

variations in capped samples were used to obtain an equivalent scale in monolayers (MLs) deposition for this technique [17]. This allowed determination of the 2-D to 3-D transitions for $In_{0.6}Ga_{0.4}As$/GaAs in a similar fashion as reported by Leonard et al.[19] and Kobayashi et al.[20] for InAs/GaAs. Our experiments demonstrate a similar exponential behavior in ternary InGaAs/GaAs dot formation. Figure 3 shows the island concentrations as a function of deposition in an equivalent monolayers (ML) scale for conditions of high and low Arsine partial pressures. Curves (a) and (b) were obtained at different values of Arsine partial pressure, at the values indicated by hollow arrows in Figure 1. As can be seen, different critical thicknesses for the S-K transition are obtained depending on Arsine partial pressure. A smaller critical thickness is obtained at high values of Arsine partial pressure, indicating that high Arsine flows can partially suppress, or at least delay the S-K transformation. Similar growth suppression effects have been reported for InGaAs films grown by molecular beam epitaxy, in which 2-D growth could be maintained to higher depositions at lower temperatures [15]. The island concentration curves shown in figure 3 indicate that different values for the 2-D to 3-D transition can be obtained in InGaAs/GaAs, depending on growth conditions.

In the next experiment, both growth and annealing of the InGaAs islands was executed under different Arsine partial pressures, indicated by arrows (a) and (b) in figure 1. Annealing times were 60 minutes in both cases. The morphologies of the sample surfaces after such anneals are shown in Figure 4. Figure 4 (a, b, and c) shows the results for anneals at high Group V partial pressures and 4 (d, e and f) for low arsine partial pressures. As can be seen, the differences in morphology are rather dramatic. All other growth conditions such as temperature, impurities, $H_2$ flow, deposition times and growth rates were identical. As can be seen, coverages are lower and the size and density of large islands is higher than in 4 (d, e, f), which shows the results of growth and a 60 minute anneal in $10^{-6}$ arsine partial pressure. The differences indicate that significant ripening has occurred in the first case, while negligible ripening is seen in the other case.

Several features can be seen from figures 4 (a and b). The most prominent are the large dome-shaped islands. Vertical height measurements show these to have 10 times higher aspect ratios than the uniform lens-shaped islands shown in 4(d, e and f). As seen in 4 (c), these are faceted, with similar dome-like structure as reported by Medeiros et al. for the growth of Si-Ge islands [9] and assumed by Ross et al. during TEM observation of in-situ ripening [7]. Other features were much flatter, best observed by FM. The latter faceted elongated hexagonal islands and unformed large flat islands are also shown in figure 4 (a) and 4 (b). The observation of different types of islands indicates that the system was still under ripening after 1 hr anneal. No such structures were observed in the annealing conditions under low arsine partial pressures growth, instead, these conditions produced islands in high concentrations, good size and shape uniformity, and smooth, continuously curved surfaces. The latter was verified by high resolution SEM and by FM using low cone angle tips.

Large islands are not present when the small islands show the largest coverage; however, at arsine flows above and below this "optimum" value for maximum island coverage, large islands were observed even though the deposition for the S-K transformation was not exceeded. This agrees with our observation of ripening at high arsine partial pressures, where the large domed islands shown in figure 4(c) are most likely a later stage of the large dislocated islands shown in figure 2, which ripened at the expense of the smaller islands. The variation in average diameters for these large islands as a function of arsine partial pressures indicates the possibility that ripening and accelerated growth for incoherent islands is already occurring during sample cooling. Larger incoherent islands experience a higher rate of growth. Such accelerated growth for strain relaxed islands was observed in the Ge/Si(100) system by Krishnamurthy et al. [21] and later explained by Drucker [22] from differences between chemical potentials in strained and unstrained islands. Such dissimilar rates of growths have the effect of making the bimodal distribution in sizes more pronounced. This effect is also observed

in InGaAs/GaAs island growth and it is illustrated in figure 5, which shows a growth under the same arsine partial pressure conditions as used for the islands in figure 2, but where the growth was stopped shortly after the S-K transformation in 5(a), and after an additional 2 ML deposition [5(b)].

From figure 1 it can be seen that maximum island coverage is obtained with an "optimal" value for $AsH_3$ partial pressure. The island coverage rises to its maximum value at $AsH_3$ partial pressures around $10^{-6}$, and decreases again to a very low value at high $AsH_3$ partial pressures. In determining the causes for such variability it must be considered that different mechanisms might play a role on the island concentration shown on the right and left sides of the maximum value for coverage in figure 1. At very low group V partial pressures, the possibility of group III reconstructed surfaces and their known effects on adatom mobilities must be considered. However, changes in reconstruction are not detectable during MOCVD growth.

We have shown here that a large variation in island density results from changing the $AsH_3$ concentration, furthermore, dramatic differences are seen upon annealing. Our results also indicate that a later onset of the S-K transformation is observed with the same conditions that promote low surface coverage, and that the conditions that promote low island densities also result in metastable island configurations causing ripening even during cooling with no annealing. These results can be explained using energetic, rather than kinetic considerations. The differences in island coverage can be explained by considering the thermodynamic driving force in S-K island formation.

In the formation of coherent S-K islands a reduction in strain energy is achieved at the expense of an increase in surface energy. The change in energy with formation of one island can be expressed as:

$$\Delta E_{isl} = \Delta E_{surf} + \Delta E_{ela}$$

where $\Delta E_{surf}$ is the cost in surface energy and $\Delta E_{ela}$ is the change in strain energy due to elastic relaxation. It is easy to see that if the surface energy is lowered, island formation will be promoted for a fixed value of bulk elastic energy. Therefore, a decrease in island coverage suggests an increase in surface energy, with the surprising result that Arsine can be used as an impurity free "surfactant". In S-K systems, impurities that raise surface energies were called "morphactants" by Eaglesham et al. [14] who found that different shapes were obtained during prolonged annealing experiments with the addition of different impurities used as surfactants in Ge/Si strained island growth. Interestingly, it appears than Arsine at large overpressures can act in an analogous manner in the growth of III-V. Prolonged annealing under high $AsH_3$ pressures then decreases the island density and induce facetting as expected. This explanation is supported not only by effects in island surface coverage, but also by our annealing experiments.

Coarsening or Ostwald ripening have been predicted for unstable or metastable configurations [22] with no ripening if the system is in equilibrium. Therefore we believe that the arsine flows that produce the highest density of small islands can be used to achieve equilibrium for growth of InGaAs islands on GaAs (100), since ripening is not observed even under prolonged annealing. Furthermore, our results indicate that lens-shaped islands can be the equilibrium configuration for InGaAs/GaAs strained coherent islands.

In conclusion, InGaAs/GaAs(100) island growth experiments done at different value of arsine partial pressure have shown that arsine can partially suppress the S-K transformation and drastically reduce island coverages. It was found that the same conditions that promote low island coverage also cause a later onset of the S-K transformation, resulting in thicker films before island formation is observed. We have also shown that it is possible to achieve thermodynamically stable smooth unfacetted island growth when surface energies are minimized in the growth of InGaAs.

REFERENCES

*Part of this work was performed while at the Research School of Physical Sciences and Engineering, Australian National University, Canberra, ACT 0200, Australia

1. D. J. Eaglesham and M. Cerrullo, Phys. Rev. Lett. 64, 1943 (1990).
2. S. Guha, A. Maduhkar, and K. C. Rajkumar, Appl. Phys. Lett 57, 2110 (1990).
3. C. W. Snyder, B. G. Orr, D. Kessler, and L. M. Sander, Phys. Rev. Lett. 66, 3032 (1991).
4. D. Leonard, M. Krishnamurthy, C. M. Reaves, S. P. Denbaars, and P.M. Petroff, Appl. Phys. Lett. 63, 3203 (1993).
5. J. M. Moison, F. Houzay, F. Barthe, L. Leprince, E. Andre, and O. Vatel, Appl. Phys. Lett., 64, 196 (1994).
6. R. Notzel, J. Temmyo, and T. Tamamura, Nature 369, 131 (1994).
7. F. M. Ross, J. Tersoff, and R. M. Tromp, Phys. Rev. Lett. 80, 984 (1998).
8. T. I. Kamins, E. C. Carr, R.S. Williams, and S. J. Rosner, J. Appl. Phys. 81, 211 (1997).
9. G. Medeiros-Ribeiro, A. M. Bratkovski, T. I. Kamins, D. A. A. Ohlberg, and R. S. Williams, Science 279, 353 (1998).
10. B. D. Min, Yong Kim, E. K. Kim, S-K Min, and M. J. Park, Phys. Rev. B (in press).
11. M. Copel, M. C. Reuter, E. Kaxiras, and R. M. Tromp, Phys. Rev. Lett. 63, 632 (1989).
12. F. K. LeGoues, M. Copel and R. M. Tromp, Phys. Rev. Lett. 63, 1826 (1989).
13. Y. Kumagai et al., Jpn. J. Appl. Phys. 35, L476 (1996).
14. D. J. Eaglesham, F. C. Unterwald, and D. C. Jacobson, Phys. Rev. Lett. 70, 966 (1993).
15. C. W. Snyder, J. F. Mansfield, and B. G. Orr, Phys. Rev. B 46, 9551 (1992).
16. R. Leon, T. J. Senden, Yong Kim, C. Jagadish, and A. Clark, Phys. Rev. Lett 78, 4942 (1997).
17. R. Leon and S. Fafard, Phys. Rev. B (in press).
18. R. Leon, C. Lobo, and A. Clark, R. Bozek, A. Wysmolek, A. Kurpiewski, and M. Kaminska, J. Appl. Phys. (in press).
19. D. Leonard, K. Pond and P. M. Petroff, Phys. Rev. B 50, 11 687 (1994).
20. N. P. Kobayashi, T. R. Ramachandran, P. Chen, and A. Madhukar, Appl. Phys. Lett. 68, 3299 (1996).
21. M. Krishnamurthy, J. S. Drucker, and J. A. Venables, J. Appl. Phys. 69, 6461 (1991).
22. J. Drucker, Phys. Rev. B 48, 203 (1993).
23. V. A. Shchukin, N. N. Ledentsov, P. S. Kop'ev, and D. Bimberg, Phys. Rev. Lett. 75, 2968 (1995).

FIGURE CAPTIONS

Figure 1. Variations in small (35-45 nm diameter) InGaAs island coverages as a function of $AsH_3$ partial pressure. Growth temperature was 550 °C and the deposition was nominally 5 ML at a growth rate of 0.5ML per second. Hollow arrows labeled (a) and (b) indicate the partial pressures used in the evolution of island concentrations shown in figure 3. Variation in diameter for large islands and their fractional surface coverages are also shown.

Figure 2. Plan view TEM micrograph showing the morphology of the islands grown under the same conditions as in (a), (b) and (c) but without annealing or growth interruption after island formation. TEM shows the larger islands to be incoherent.

Figure 3. Island concentration as a function of deposition using MOCVD conditions that produce a graded growth rate. (a) at low $AsH_3$ partial pressure favoring high island coverages, and (b) higher $AsH_3$ partial pressure producing lower island coverage and a larger proportion of large islands.

Figure 4. Surface morphologies after 60 minutes anneals under high $AsH_3$ flows. (a) and (b) are deflection FM images and (c) is a high resolution SEM image of dome shaped islands not resolved with etched silicon nitride tips. (d), (e) and (f) show morphologies of sample grown under the same conditions and annealed for 60 minutes under the low $AsH_3$ flow producing maximum island densities shown in figure 1. (d) and (e) are deflection FM images and (f) is a high resolution SEM micrograph.

Figure 5. InGaAs/GaAs evolution in bimodal behavior for deposition beyond saturation island densities. Shown for two different growths at 17 slm of $H_2$. Estimated deposition: a) 5.5 ML. b) 7.5 ML.

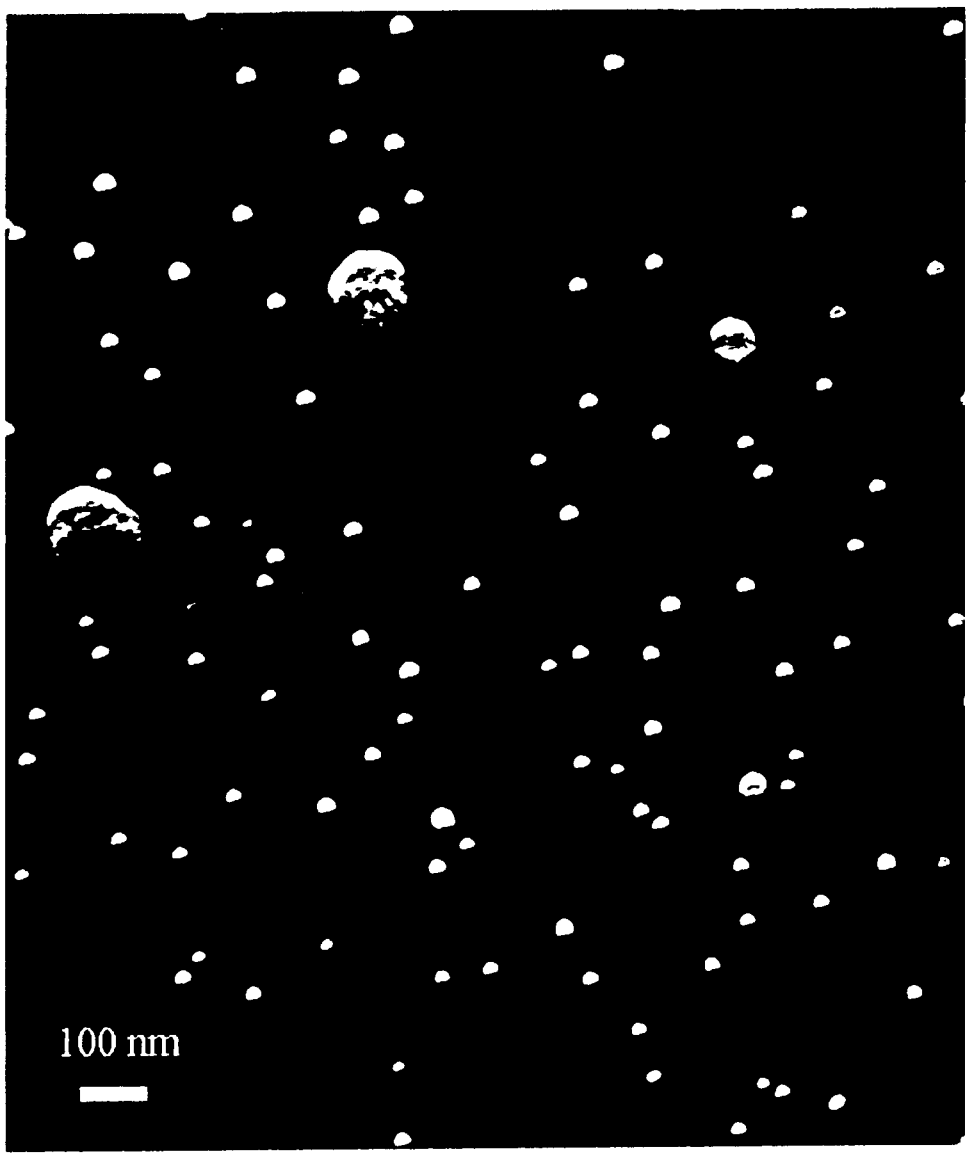
100 nm

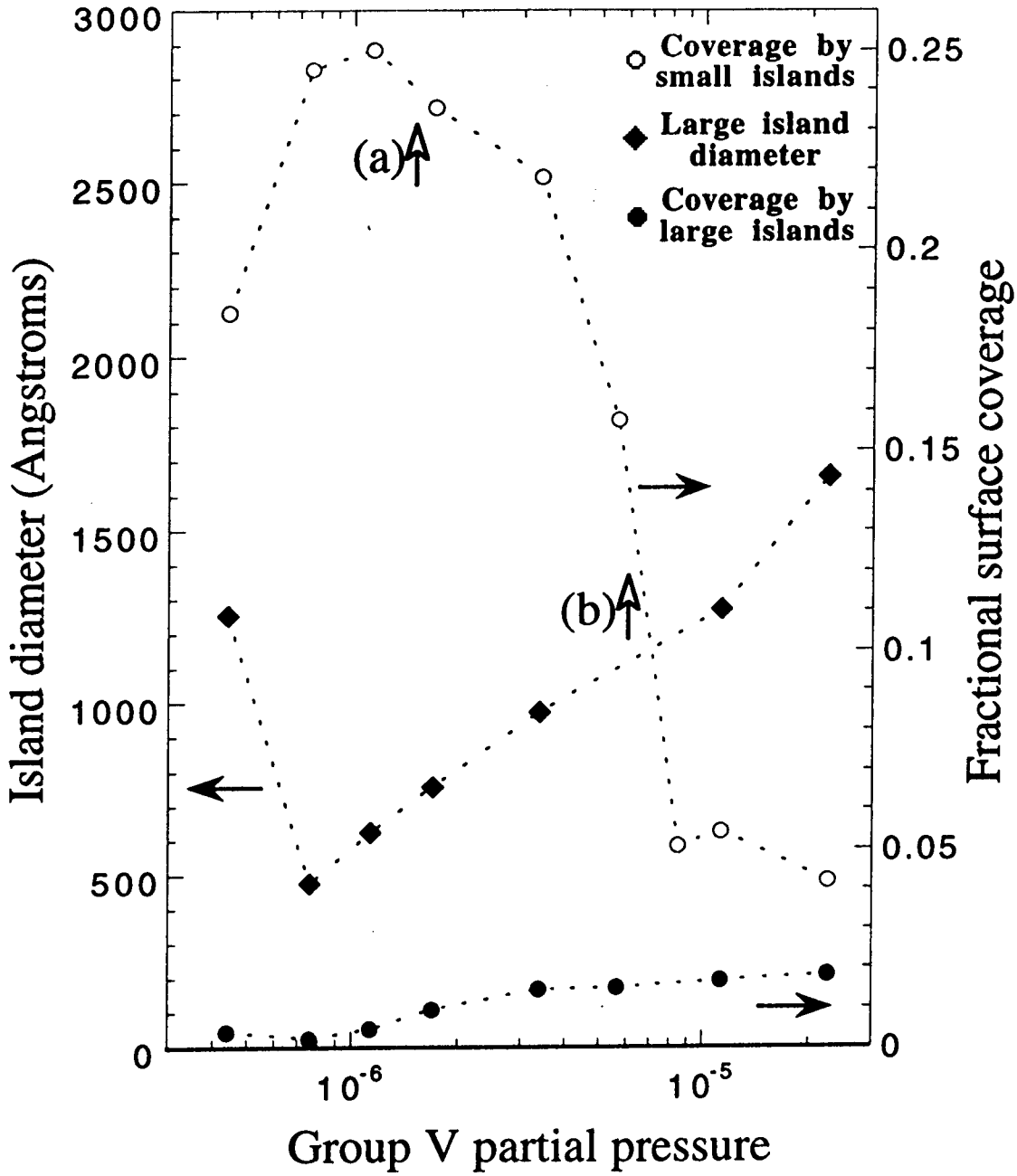
3000
2500
2000
1500
1000
500
0
0.25
0.2
0.15
0.1
0.05
0
Coverage by small islands
Large island diameter
Coverage by large islands
(a)
(b)
Island diameter (Angstroms)
Fractional surface coverage
$10^{-6}$
$10^{-5}$
Group V partial pressure

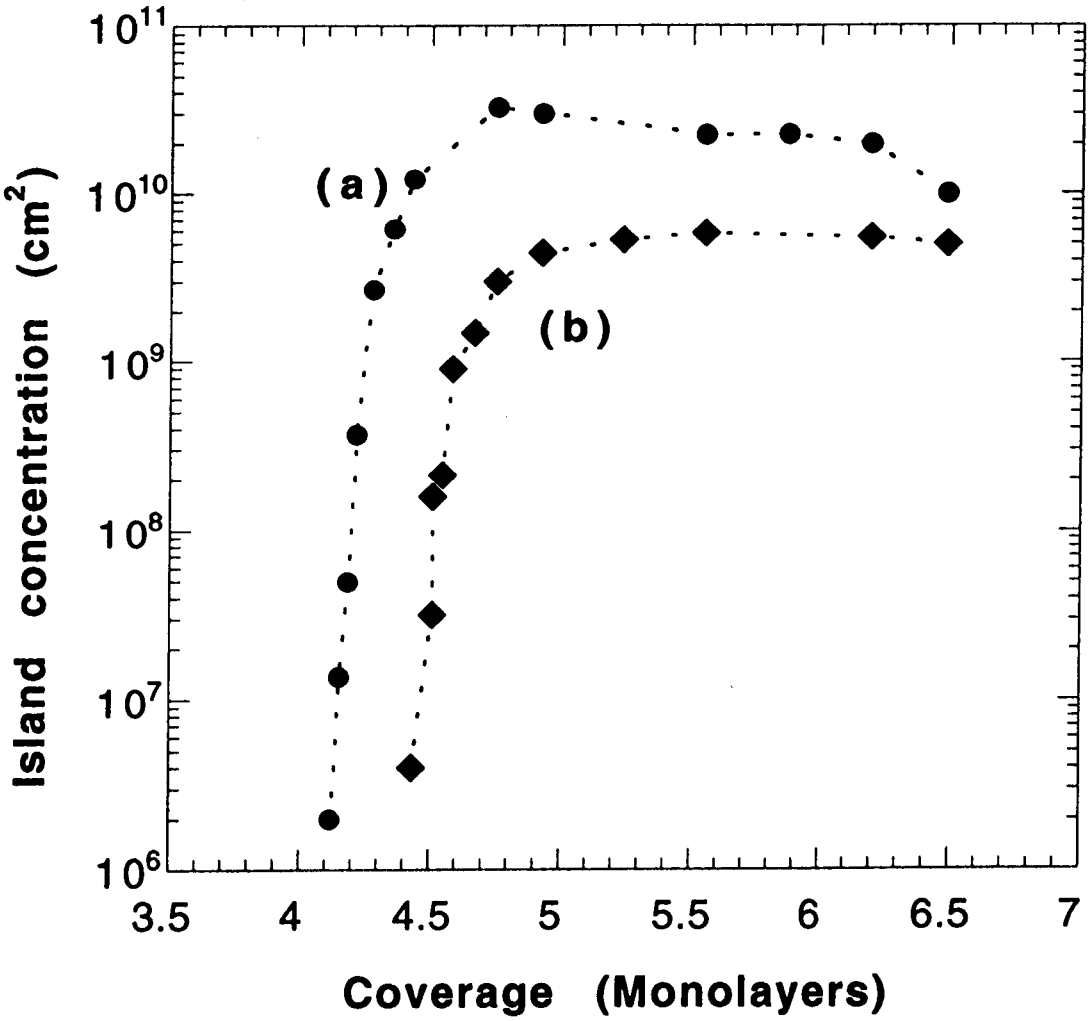
Island concentration (cm$^2$)
$10^{11}$
$10^{10}$
$10^9$
$10^8$
$10^7$
$10^6$
(a)
(b)
3.5
4
4.5
5
5.5
6
6.5
7
Coverage (Monolayers)

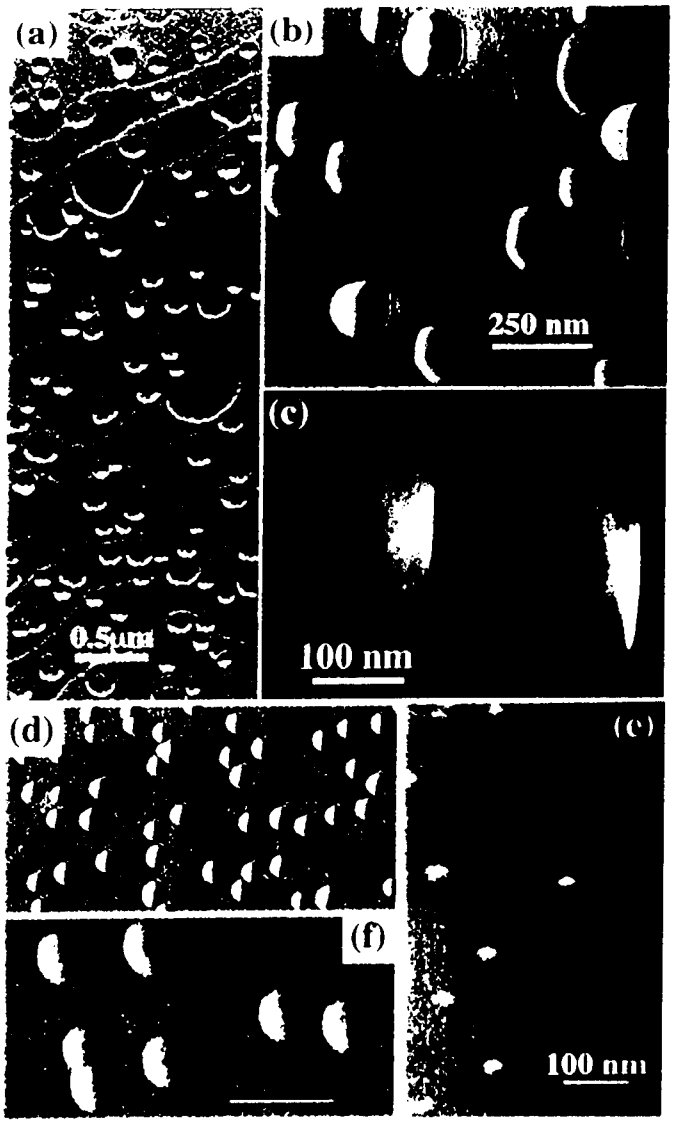
(a)
0.5um
(b)
250 nm
(c)
100 nm
(d)
(f)
(e)
100 nm

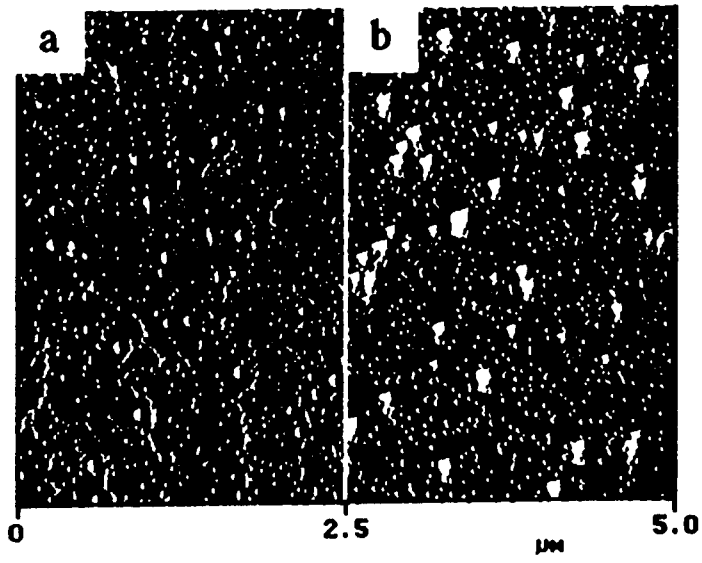
a
b
0
2.5
5.0
μm